Available online at www.sciencedirect.com
ScienceDirect
Carbohydrate Research 343 (2008) 919–928
Carbohydrate RESEARCH

Effect of solvent exchange on the supramolecular structure, the molecular mobility and the dissolution behavior of cellulose in LiCl/DMAc

Daisuke Ishii,[†] Daisuke Tatsumi[*] and Takayoshi Matsumoto

Division of Forest and Biomaterial Science, Graduate School of Agriculture, Kyoto University, Kitashirakawa Oiwake cho, Sakyo-ku, Kyoto 606-8502, Japan

Received 12 April 2007; received in revised form 22 January 2008; accepted 23 January 2008
Available online 2 February 2008

Abstract—We investigated the effect of solvent exchange on the supramolecular structure and the molecular mobility of the cellulose molecule to clarify the mechanism of the dissolution of cellulose in lithium chloride/*N*,*N*-dimethylacetamide (LiCl/DMAc). Among the celluloses that were solvent exchanged in different ways, the DMAc-treated celluloses dissolved most rapidly. Dissolution of the acetone-treated celluloses was much slower than the DMAc-treated ones, but considerably faster than the untreated one. Such differences in the dissolution behavior were well explained by the differences in the surface fractal dimension calculated from the small-angle X-ray scattering profiles and in the ^{1}H spin–lattice and spin–spin relaxation times estimated from the solid-state NMR spectroscopic measurements. Furthermore, it was suggested from the IR spectra and the ^{13}C spin–lattice relaxation times of cellulose that DMAc is adsorbed on the surface of cellulose even after vacuum-drying and affects the molecular mobility and hydrogen-bonding state of cellulose.

Keywords: Cellulose; LiCl/DMAc; Solvent exchange; Supramolecular structure; Solid-state NMR spectroscopy; SAXS

1. Introduction

Cellulose is one of the most abundant biological polymers available to humans. While cellulose is used in the form of fabrics and yarns, it is also used as a raw material for making films, fibers, and molded materials. Furthermore, various cellulose derivatives have been developed to improve the mechanical and thermal properties of cellulose. Dissolution of cellulose is indispensable throughout these processes, because cellulose itself is not a thermoplastic material. Therefore, many kinds of cellulose solvents have been developed and industrially used. However, most of the conventional cellulose solvents contain harmful and/or volatile substances that cause environmental pollution. Because of these shortcomings, processing of cellulose from the dissolved state has been limited. From the 1980s, various kinds of novel cellulose solvents have been developed to overcome the problems of conventional cellulose solvents. Lithium chloride/*N*,*N*-dimethylacetamide (LiCl/DMAc) is one of those newly developed cellulose solvents.[1,2] This solvent can dissolve cellulose with a molecular weight of more than 10^6 under ambient conditions without severe degradation or other undesirable reactions.[3] Owing to these advantages, LiCl/DMAc has been utilized in an analytical use to investigate the molecular properties of cellulose, such as the chain dimension and flexibility

* Corresponding author at present address: Department of Forest and Forest Products Sciences, Faculty of Agriculture, Graduate School of Kyushu University, 6-10-1 Hakozaki, Higashi-ku, Fukuoka 812-8581, Japan. Tel./fax: +81 92 642 2998; e-mail: tatsumid@agr.kyushu-u.ac.jp
† Present address: Paper Science Laboratory, Department of Biomaterials Science, Graduate School of Agricultural and Life Sciences, The University of Tokyo, 1-1-1 Yayoi, Bunkyo-ku, Tokyo 113-8657, Japan.

0008-6215/$ - see front matter © 2008 Elsevier Ltd. All rights reserved.
doi:10.1016/j.carres.2008.01.035

in the dissolved state.[2,4–6] It has also been utilized as a medium for derivatizing cellulose under homogeneous conditions.[7] Control of the degree of substitution and chemical structure (regiospecificity) of cellulose derivatives has been realized by using this solvent system.

Several different methods have been developed for the dissolution of cellulose in LiCl/DMAc. Among them, a solvent exchange procedure is generally employed to dissolve cellulose in LiCl/DMAc.[1,2] This procedure consists of the immersion of cellulose in water and the subsequent exchange of water in the cellulose by acetone and further by DMAc. Some researchers have explained the effect of solvent exchange as 'activation'.[1] As a phenomenological approach, Pionteck et al. investigated the effect of solvent exchange by observing the morphological changes of the cellulose solid during the dissolution in LiCl/DMAc using microscopic methods.[8] However, the mechanism on how the 'activation' affects the supramolecular structure of cellulose is still unknown. To clarify the mechanism, we have employed small-angle X-ray scattering and solid-state NMR spectroscopy to investigate the changes in the nanometer-scale heterogeneity in the solid structure and molecular mobility.[9,10] As a result, we have shown that the solvent exchange affects the molecular mobility and the 100 nanometer-order heterogeneity of cellulose. Such length scale corresponds to the 'level-off degree of polymerization'[11] of cellulose, known as a kind of dynamic heterogeneity in cellulose solid. Nevertheless, several questions remain unresolved on the effect of solvent exchange on cellulose. One question is why the sequential immersion using water and some kinds of organic liquid is required. Another question is what kind of molecular motion of cellulose is affected by the solvent exchange. Following our previous investigation, small-angle X-ray scattering (SAXS) measurements were performed to investigate the nanometer-order structure of cellulose. In addition, the measurements of T_{1H} (laboratory-frame ^{1}H spin–lattice relaxation time) and T_{2H} (^{1}H spin–spin relaxation time) were also performed to investigate the dynamic heterogeneity of cellulose. As translation of the molecular chain is impossible in the solid state, it is supposed that the rotation and/or the vibration of the specific sites in the cellulose molecule are affected by the solvent exchange.

Solid-state NMR[12–15] and infrared (IR) spectroscopy[16–21] can give the information on the motional state of the specific sites in the cellulose molecule. However, the relation between the motional state of the molecule and the solubility of cellulose has not yet been clarified. Therefore, we performed the measurements of ^{13}C spin–lattice relaxation time (T_{1C}) and the Fourier-transform (FT) IR spectra to investigate the effects of solvent exchange on the motional state of the cellulose molecule.

2. Experimental

2.1. Sample preparation

Cellulose material employed was softwood sulfite pulp of dissolving pulp grade (DP, Nippon Paper Industry Co., Ltd). After vacuum-drying at 60 °C for 24 h, the cellulose was treated in either of the following ways: immersion in water followed by exchange to acetone and the further exchange to DMAc (sample A); immersion in water followed by exchange to acetone (sample B); immersion in water followed by exchange to DMAc (sample C); immersion in acetone followed by exchange to DMAc (sample D); immersion in acetone (sample E); immersion in DMAc (sample F). Water was deionized from tap water to an electrical conductivity of less than 0.2 $\mu S\,cm^{-1}$ and further distilled in the laboratory. Reagent-grade acetone, DMAc, and LiCl were purchased from Nacalai Tesque, Japan and were used without further purification. While the immersion in water was performed once for 2 days, the immersion in acetone or DMAc was performed for 1 day and repeated twice. About 10 g of cellulose samples were immersed in 100 mL of water, acetone, or DMAc at room temperature. After the above-mentioned treatments, these celluloses were vacuum-dried again at 60 °C for 40 h. In addition to the solvent-exchanged celluloses, decrystallized cellulose was prepared by cryogenic milling using a Japan Analytical Chemistry AFC-300 cryogenic sample crusher.[9] None of the solvent-exchange procedures applied to samples A to F were applied to the milled cellulose.

2.2. Dissolution of cellulose

The cellulose samples were mixed with 8 wt % LiCl/DMAc at a ratio of 3:97 (w/w), and the mixtures were allowed to stand at room temperature. When the visible turbidity or solid residues were lost from the mixture, we regarded that the dissolution of cellulose was completed.

2.3. Small-angle X-ray scattering (SAXS)

A 6-m point-focus SAXS camera at the High-Intensity X-ray Laboratory of Kyoto University was utilized.[22] The sample-to-detector distance was set to 1.6 m, covering the real-space length scales between 3 and 40 nm. A scattered intensity of Cu Kα irradiation ($\lambda = 0.1542$ nm, 40 kV, and 50 mA) was acquired using two-dimensional position-sensitive proportional counter for more than 5000 s. The two-dimensional scattering profiles so obtained were corrected for the transmittance in the samples, the incident beam intensity (calibrated using high-density polyethylene as secondary standard), and the background intensity from air scattering and electronic noise. By circularly averaging the corrected two-dimensional profiles, one-dimensional profiles were finally obtained.

2.4. CP/MAS ^{13}C solid-state NMR spectroscopy

Solid-state NMR spectroscopic measurements were performed using a Chemagnetics CMX300 Infinity spectrometer. The resonance frequency for ^{1}H and ^{13}C was 296.9 ppm and 74.7 ppm, respectively. A 90° pulse width for ^{1}H and ^{13}C, a contact time for CP, and a delay time after the acquisition of FID were 5.5 μs, 1 ms, and 6 s, respectively. Hexamethylbenzene was used for the calibration of the CP amplitude, the magic angle and ^{13}C chemical shifts. ^{1}H spin–lattice relaxation time in the laboratory frame (T_{1H}) was measured using the inversion–recovery method. ^{1}H spin–spin relaxation time (T_{2H}) was measured using the spin–echo method. In these measurements, partially relaxed magnetization of ^{1}H was transferred to ^{13}C via CP. Then, the intensity of ^{13}C magnetization was recorded and analyzed as a function of the delay time for the relaxation of ^{1}H magnetization. The ^{13}C spin–lattice relaxation time (T_{1C}) measurement was performed using Torchia's CPT1 sequence.[23]

2.5. FTIR spectroscopy

A Shimadzu FTIR8200 spectrometer equipped with a diamond ATR accessory (DuraSamplIR II, SensIR Technologies) was used for the FTIR measurements. A total of 100 scans of interferograms ranging from 600 to 5000 cm^{-1} with the resolution of 2 cm^{-1} were acquired at room temperature.

3. Results

3.1. Dissolution of cellulose

The cellulose samples treated by DMAc (samples A, C, D, and F) dissolved in LiCl/DMAc within a few hours. On the other hand, the dissolution of the untreated one was extremely slow (solid residues were observed in the mixture even after more than a year). Dissolution of the celluloses treated by acetone (samples B and E) was also much slower than those treated by DMAc, but a little faster than that of the untreated one. The acetone-treated celluloses just after the preparation completely dissolved in several weeks. However, when the acetone-treated cellulose after the storage in a desiccator with a relative humidity of about 10–30% was used, the dissolution was incomplete. In contrast, the dissolution behavior of the DMAc-treated celluloses was not significantly affected by the storage conditions. Milling did not facilitate the dissolution of cellulose at all.

3.2. SAXS measurements

The SAXS measurements were performed to investigate the nanometer-order structure of cellulose. Figure 1 shows the SAXS profiles of the cellulose samples. The relation between the scattered intensity, $I(q)$, and the magnitude of the scattering wave vector, $q = (4\pi/\lambda)\sin(\theta/2)$ (θ, the scattering angle), obeys the power law in the q range between $0.16 < (q/nm^{-1}) < 0.34$. Namely,

$$I(q) \sim q^{-D_m},\ 1 \leqslant D_m \leqslant 3 \quad \text{for mass fractals} \qquad (1)$$

and

$$I(q) \sim q^{-(6-D_s)},\ 2 \leqslant D_s < 3 \quad \text{for surface fractals} \qquad (2)$$

where D_m and D_s denote the mass and the surface fractal dimensions.[24] Values of D_m (only for sample A) and D_s are shown in Table 1. The DMAc-treated cellulose has larger fractal dimensions than the other samples. This shows that the DMAc treatment increases the surface roughness of cellulose at the nanometer scale.

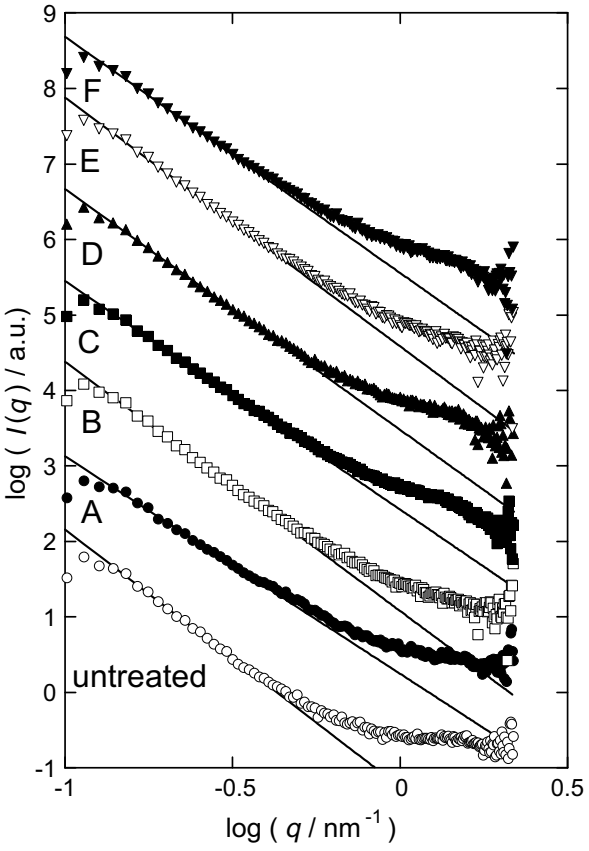

Figure 1. SAXS profiles of celluloses. Filled symbols of the samples A, C, D, and F indicate the samples treated by DMAc.

3.3. Solid-state NMR spectroscopy

The solid-state NMR spectroscopic measurements were performed to investigate the dynamic heterogeneity and the motional state of the cellulose molecule. First, we performed ^{1}H spin–lattice (T_{1H}) and spin–spin (T_{2H}) relaxation time measurements for the evaluation of the

Table 1. Fractal dimensions and NMR ^{1}H spin–relaxation times of solid celluloses

Sample	D_m or D_s	T_{1H} (s)	T_{2H1} (μs)	T_{2H2} (μs)	L (nm)
Untreated	2.53	2.9	6.0	44	153
A[a]	2.86 (D_m)	1.8	7.7	83	107
B	2.65	2.4	7.2	46	133
C[a]	2.96	1.9	7.8	895	111
D[a]	2.74	1.8	7.1	41	111
E	2.67	2.0	7.5	84	114
F[a]	2.84	2.2	7.8	17	126
Milled[b]	2.34	2.8	6.4	387	144

[a] DMAc-treated samples.
[b] The values for the milled cellulose is quoted from the previous paper.[7]

spatial scale of the dynamic heterogeneity of cellulose solid. Figure 2 shows the relaxation profiles of the ^{1}H longitudinal magnetization of cellulose observed at the C-1 position (106 ppm). All the samples showed the relaxation behavior characterized by the single T_{1H}. The value of T_{1H} was calculated according to the following expression:

$$M_{LH}(t) = M_{LH}(0)\{1 - 2\exp(-t/T_{1H})\} \quad (3)$$

where $M_{LH}(t)$ denotes the intensity of longitudinal ^{1}H magnetization at the time t. ($t = 0$ represents the equilibrium state.) Figure 3 shows the relaxation profiles of the transverse magnetization of cellulose protons. The relaxation profile was decomposed into Gaussian and exponential components.[9,25] Namely,

$$M_{TH}(t) = M_{TH1}(0)\exp\{-(t/T_{2H1})^2\} + M_{TH2}(0) \times \exp(-t/T_{2H2}) \quad (4)$$

where $M_{TH}(t)$ denotes the intensity of ^{1}H transverse magnetization. Numerical 1 and 2 represent the rigid and mobile components, respectively. Using the values of T_{1H} and T_{2H}, the maximum diffusive path length, L, was calculated according to the following equation:[26]

$$L \cong (6DT_{1H})^{1/2} \quad (5)$$

where D is spin diffusion coefficient and calculated by[27]

$$D = 0.13a^2/T_{2H} \quad (6)$$

where a represents the internuclear distance between protons (0.25 nm in β-D-glucose: calculated using MOLDA software[28]). The values of T_{1H}, T_{2H}s (T_{2H1} and T_{2H2}), and L are shown in Table 1. Here, the value of T_{2H1} was used for the calculation of L. It was found that the DMAc-treated celluloses (samples A, C, D, and F) have smaller values of T_{1H}, larger values of T_{2H1}, and consequently smaller values of L than the other samples. This shows that the DMAc treatment enhanced the changes in the amplitudes of the vibration of specific bonds or functional groups in the cellulose molecule.

Next, we performed ^{13}C spin–lattice relaxation time (T_{1C}) measurements to evaluate the mobility of specific part in the cellulose molecule. Figures 4 and 5 show the relaxation profiles of ^{13}C longitudinal magnetization

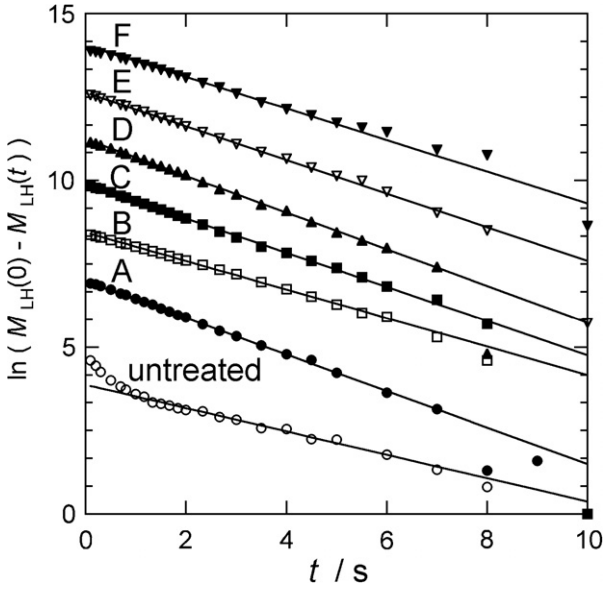

Figure 2. Laboratory-frame ^{1}H spin–lattice relaxation profiles of celluloses. Symbols are the same as in Figure 1.

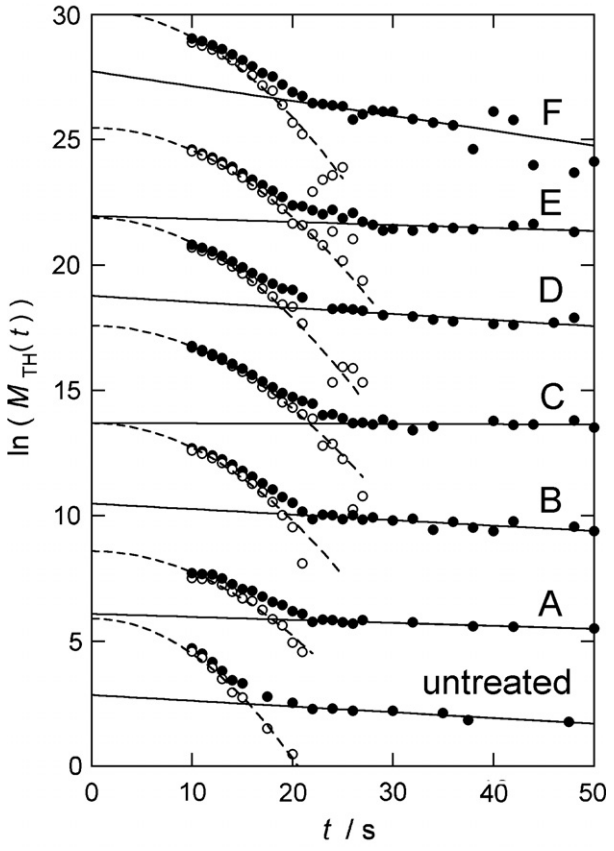

Figure 3. ^{1}H spin–spin relaxation profiles of celluloses. Filled circles: observed intensities; open circles: Gaussian components; solid line: exponential fit; dashed line: Gaussian fit.

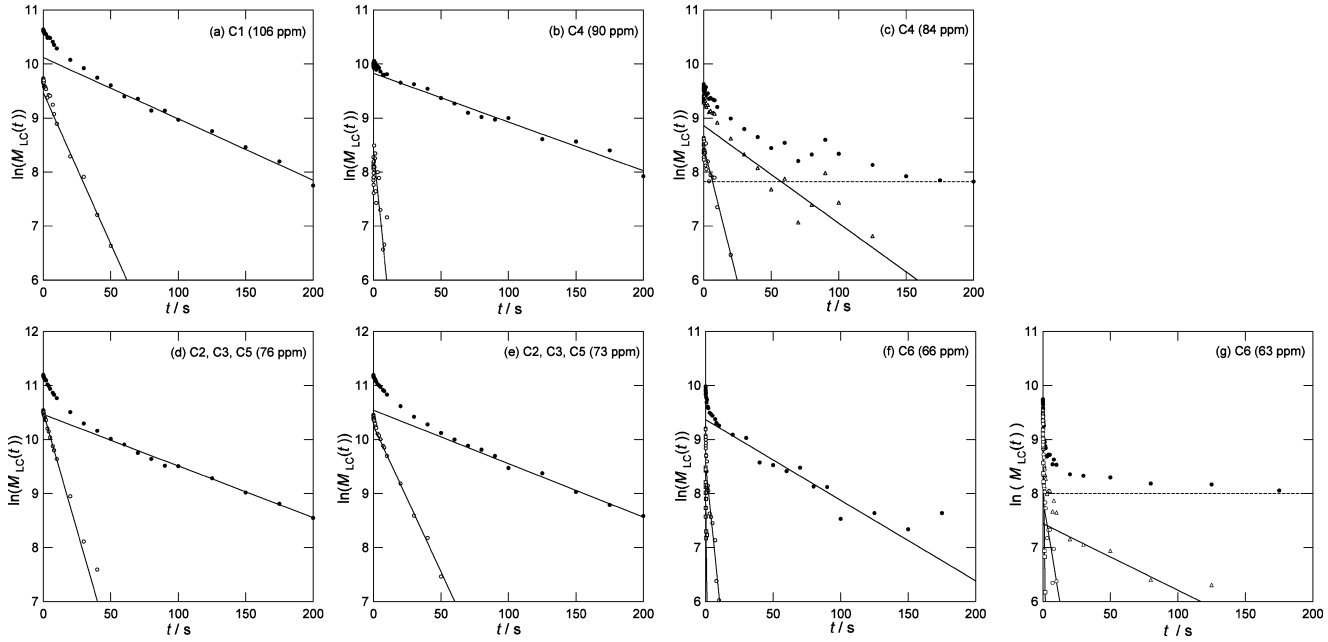

Figure 4. ^{13}C spin–lattice relaxation profiles of untreated cellulose. Filled circles: observed intensity; open triangle in (c) and (g): background-corrected observed intensity; Open circle: fast-relaxing components with the T_{1C} on the order of 10 s; open rectangle in (f) and (g): fast-relaxing components with the T_{1C} less than 1 s; solid lines: exponential fits for each relaxation components. Dashed lines in (c) and (g) represent the background intensity originating from the thermal noise.

of each carbon in cellulose.[‡] The data in Figures 4 and 5 were obtained from untreated cellulose and samples A, respectively. The data from the other samples also showed almost the same tendency. The profiles were fitted by the sum of several exponential components, which is expressed as follows:

$$M_{LC}(t) = \sum_i M_{LCi}(t) \exp(-t/T_{1Ci}) \qquad (7)$$

where $M_{LC}(t)$ and i denote the intensity of ^{13}C longitudinal magnetization and number of relaxation processes, respectively. The estimated values of T_{1C}s and the fraction of each relaxation components are shown in Table 2. In this table, fractions of each component were estimated as the ratio $M_{LCi}(0)/\sum_i M_{LCi}(0)$, shown in the parentheses. Except for the C-6 signals, the relaxation profiles of each of the resonance lines were generally decomposed into two components ($i = 2$). On the other hand, each of two C-6 signals (at 66 and 63 ppm) contained three relaxation components ($i = 3$). It was found that the DMAc-treated samples have relatively smaller T_{1C}s at 84 ppm and larger ones at 106 ppm than the other samples.

To investigate the relation between the ^{13}C spin–lattice relaxation behavior and the crystallinity of cellulose, T_{1C} measurement was also performed for the milled cellulose. It has already been shown that the milled cellulose does not show any significant crystalline peaks in the X-ray diffractogram and in the CP/MAS ^{13}C NMR spectrum.[9] Only one T_{1C} was calculated from the C-4 signal at 84 ppm. In contrast, the relaxation profiles of the signals at 75 and 63 ppm consisted of two or three components. Furthermore, the T_{1C} values of these components were comparable to those in the 'crystalline' cellulose. Considering that these signals are assigned to the C-2, C-3, and C-6 carbons at which the adjacent hydroxyl group forms a hydrogen bond, it is supposed that the hydrogen bonds exist even in the decrystallized state and restrict the motion of these carbons. The relation between the molecular mobility and the hydrogen bond is subsequently discussed in more detail.

3.4. FTIR measurements

To investigate the effect of the solvent exchange on the vibrational modes of the cellulose molecule, FTIR spectra of celluloses were obtained. Figure 6 shows the FTIR spectra of the celluloses. To clearly determine the peaks, the second derivatives of the acquired spectra were calculated. The most prominent feature of the spectrum

[‡] As for the signals at 84 ppm and at 63 ppm, the intensity was almost constant in the range of t beyond 150 s. Such leveling-off of the intensity shows that the relaxation of the magnetization of these carbons is completed. In such a case, it is supposed that only the thermal noise is detected. Therefore, as for these two signals, the intensity in the t range beyond 150 s was subtracted as background error from the intensity of the other data points in the relaxation profile. Dashed lines in Figures 4c, g and 5c represent the above-mentioned background intensity.

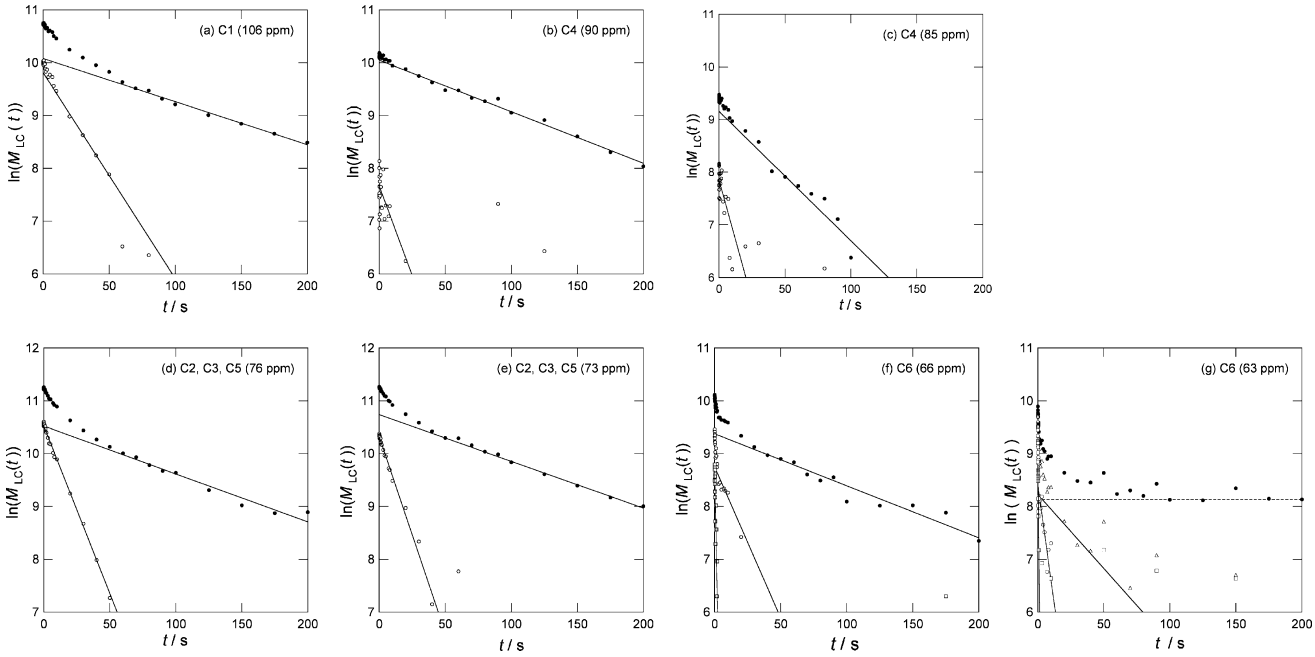

Figure 5. ^{13}C spin–lattice relaxation profiles of cellulose sample A that is treated by water, acetone, and DMAc. Symbols are the same as Figure 4.

Table 2. T_{1C} of each carbon atoms in the solid celluloses

Sample	Assignment						
	C-1 106 ppm[a]	C-4 90 ppm	C-4 84 ppm	C-2, C-3, C-5 75 ppm	C-2, C-3, C-5 73 ppm	C-6 66 ppm	C-6 63 ppm
Untreated	88 (0.72)[b] 18 (0.28)	111 (0.89) 4.1 (0.11)	55 (0.72) 10 (0.28)	105 (0.66) 11 (0.34)	101 (0.68) 18 (0.32)	67 (0.60) 4.1 (0.27) 0.5 (0.13)	81 (0.40) 6.6 (0.35) 0.6 (0.25)
A[c]	123 (0.68) 26 (0.32)	102 (0.90) 15 (0.10)	41 (0.83) 11 (0.17)	110 (0.67) 16 (0.33)	113 (0.71) 13 (0.29)	102 (0.59) 17 (0.29) 0.8 (0.12)	36 (0.17) 5.5 (0.20) 0.5 (0.63)
B	102 (0.71) 19 (0.29)	96 (1.0)	117 (0.64) 11 (0.36)	107 (0.65) 14 (0.35)	108 (0.69) 17 (0.31)	117 (0.57) 12 (0.30) 0.6 (0.13)	50 (0.17) 4.0 (0.24) 0.5 (0.59)
C[c]	113 (0.70) 14 (0.30)	127 (0.83) 17 (0.17)	42 (0.76) 13 (0.24)	120 (0.66) 15 (0.34)	120 (0.68) 18 (0.32)	98 (0.57) 13 (0.27) 0.8 (0.16)	123 (0.05) 5.4 (0.22) 0.5 (0.73)
D[c]	102 (0.70) 23 (0.30)	105 (0.87) 12 (0.13)	52 (0.68) 9.5 (0.32)	101 (0.67) 16 (0.33)	116 (0.67) 19 (0.33)	87 (0.59) 9.8 (0.29) 0.5 (0.12)	36 (0.12) 2.0 (0.25) 0.4 (0.63)
E	106 (0.71) 23 (0.29)	113 (0.84) 33 (0.16)	49 (0.76) 8.0 (0.24)	101 (0.66) 14 (0.34)	113 (0.67) 19 (0.33)	174 (0.59) 13 (0.29) 0.6 (0.12)	57 (0.25) 1.7 (0.15) 0.2 (0.60)
F[c]	120 (0.71) 14 (0.29)	119 (0.87) 18 (0.13)	44 (0.74) 6.9 (0.26)	107 (0.68) 15 (0.32)	108 (0.73) 14 (0.27)	95 (0.58) 8.7 (0.29) 0.6 (0.13)	90 (0.25) 2.8 (0.16) 0.1 (0.59)
Milled	381 (0.55) 30 (0.36) 8 (0.09)		20 (1.0)	95 (0.54) 21 (0.46)			32 (0.22) 2.0 (0.19) 0.3 (0.59)

[a] The chemical shift of the C-1 carbon in the milled cellulose is 105 ppm.[7]
[b] Values in parentheses denote the fraction of each components.
[c] DMAc-treated samples.

of the DMAc-treated cellulose is the absorption at 1616 cm^{-1}. No such absorption was observed in the untreated cellulose. Another absorption band was found at 1267 cm^{-1} only in the spectrum of the DMAc-treated cellulose. These bands are assigned to the stretching of carbonyl group (1616 cm^{-1}) and the asymmetrical

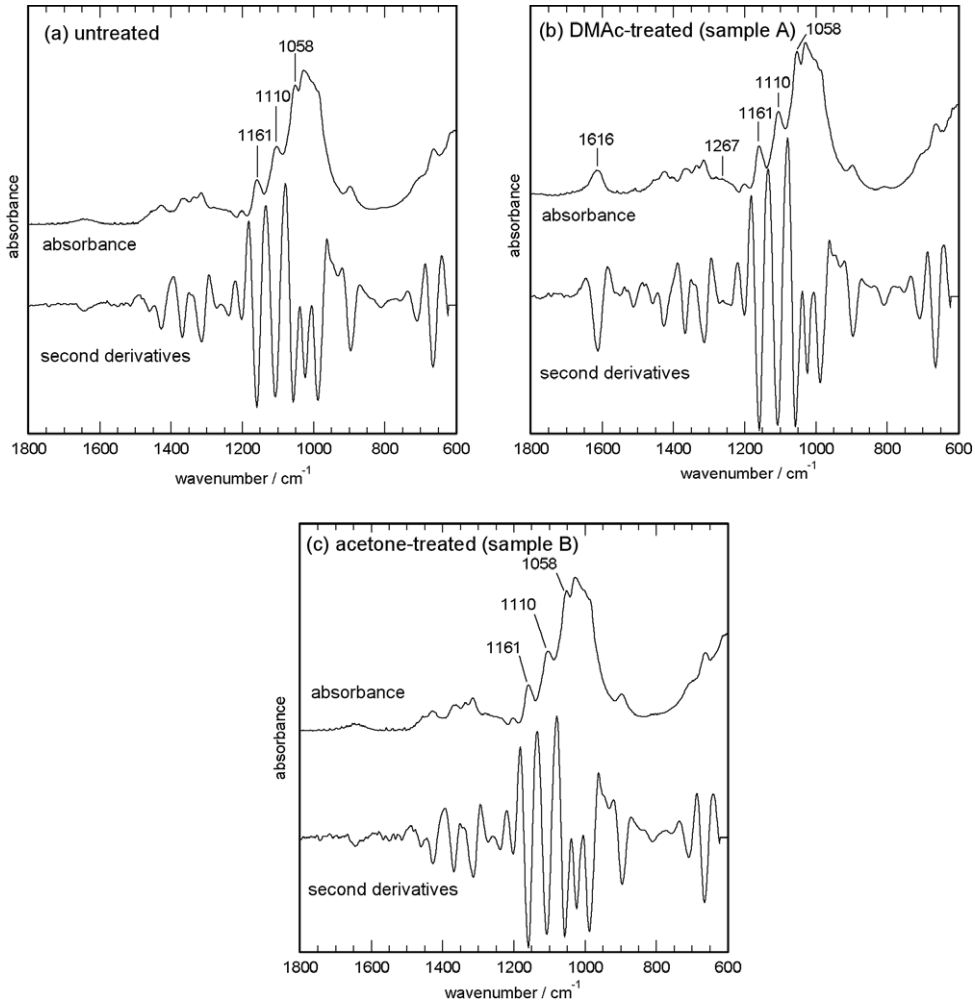

Figure 6. FTIR spectra of celluloses in the low-wavenumber regions.

stretching of the two N–C_{methyl} bonds (1267 cm^{-1}) of the DMAc molecule, respectively.[29] As the absorption of the carbonyl group shifted toward lower frequencies from that observed for the neat DMAc (Fig. 7), it is supposed that DMAc is adsorbed on the surface of cellulose.

The absorptions around 3000–3500 cm^{-1} that have been assigned to the stretching of the hydroxyl groups[16–21] were affected by the DMAc treatment. Figure 8 shows the deconvoluted IR spectra of the celluloses in the OH-stretching region. The major contributions were the absorbances at 3458, 3336, and 3267 cm^{-1}. These bands are assigned to the stretching of the hydroxyl group not hydrogen bonded (3458 cm^{-1}), that of hydrogen-bonded OH-3 (3336 cm^{-1}), and that of hydrogen-bonded OH-2 (3267 cm^{-1}), respectively.[21] The intensities of these absorption bands estimated from the deconvoluted spectra are shown in Table 3 as well as the relative values of the intensities to the absorbance at 2900 cm^{-1}. DMAc treatment significantly decreased the intensities at 3458 and 3267 cm^{-1} but increased that at 3336 cm^{-1}. Acetone treatment slightly increased the intensity at 3458 cm^{-1} and decreased those at 3336 and 3267 cm^{-1}. In the

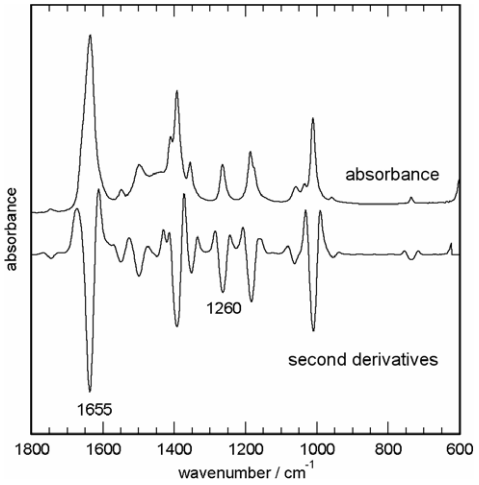

Figure 7. FTIR spectra of DMAc (neat liquid).

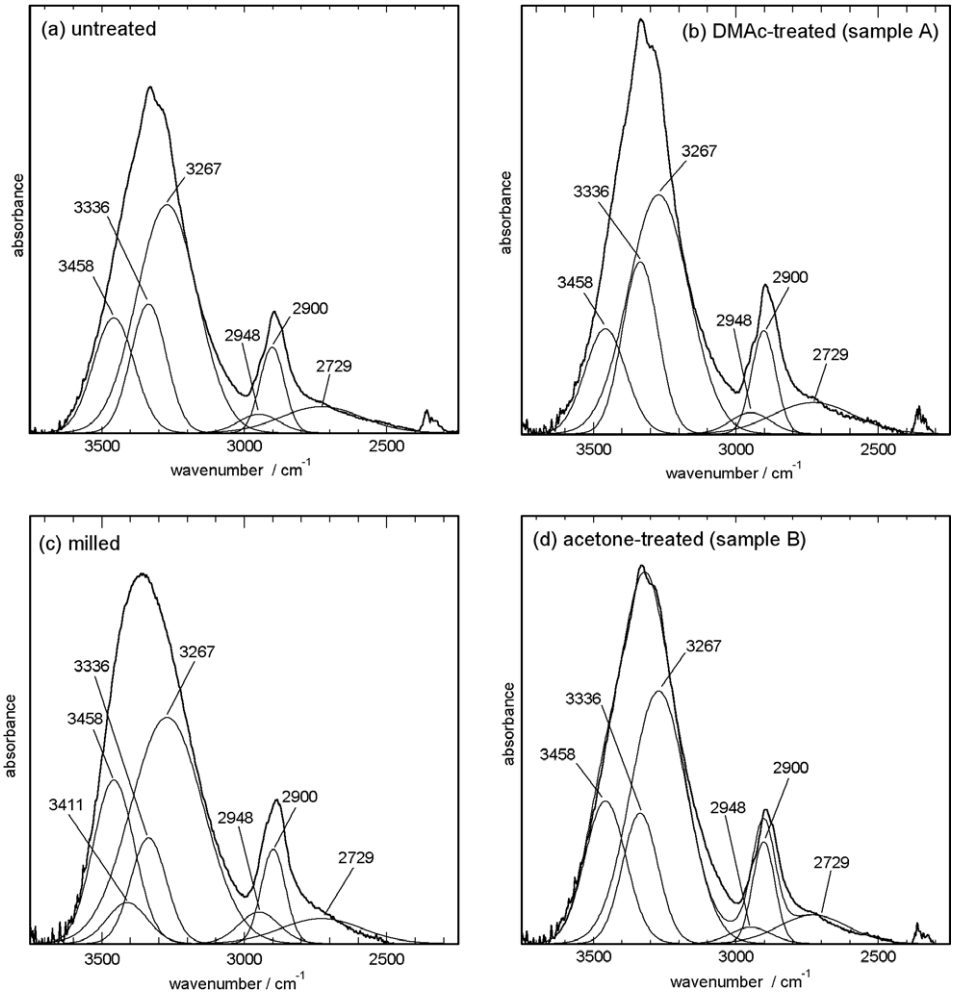

Figure 8. FTIR spectra of celluloses in the high-wavenumber regions.

Table 3. Intensities of each peak in the deconvoluted FTIR spectra of the celluloses in the OH-stretching regions

Wavenumber (cm^{-1})	Untreated	Sample A	Sample B	Milled
3458	0.042 (1.3)[a]	0.015 (1.0)	0.035 (1.4)	0.026 (1.7)
3411				0.007 (0.43)
3336	0.047 (1.5)	0.025 (1.7)	0.032 (1.3)	0.017 (1.1)
3267	0.083 (2.7)	0.035 (2.3)	0.062 (2.5)	0.036 (2.4)
2900	0.031 (1.0)	0.015 (1.0)	0.025 (1.0)	0.015 (1.0)

[a] Values relative to the absorbance at 2900 cm^{-1}.

milled cellulose, while the intensity at 3458 cm^{-1} was increased, the intensity at 3336 cm^{-1} was unaffected. The DMAc-treated cellulose showed lowest absorption at 3458 and 3267 cm^{-1}. Both of these absorptions are assigned to the stretching of the hydrogen-bonded OH group adjacent to the C-2 carbon. On the other hand, the absorption at 3336 cm^{-1}, assigned to the stretching of the OH-3 hydroxyl group forming a hydrogen bond with the O-5 oxygen atom, was the strongest in the DMAc-treated cellulose. In addition to the absorptions related to secondary hydroxyl groups, the absorption band at 3411 cm^{-1}, that is assigned to the stretching of the hydrogen-bonded OH-6 group, was observed only in the milled cellulose.

4. Discussion

In previous papers,[9,10] we have shown that the molecular mobility and the nanometer-order structure of cellulose are affected by solvent exchange. Similar effects were found in the fractal dimensions obtained from the SAXS measurements and the ^1H spin-relaxation times (T_{1H} and T_{2H}) of the DMAc-treated celluloses

(samples A, C, D, and F). That is, the DMAc-treated celluloses dissolved in the solvent remarkably faster than the other samples and have larger fractal dimensions, which means the DMAc-treated celluloses have large surface roughness.[9] Furthermore, the DMAc-treated samples have smaller T_{1H}s and larger T_{2H}s, indicating that the molecular mobility of the DMAc-treated samples is higher than that of the untreated one. These results show that the treatment by DMAc has the most impact on the solvent exchange process of cellulose.

The details of the effects of DMAc treatment on the molecular mobility of cellulose can be investigated by the evaluation of T_1 of each carbon in the cellulose molecule. In the following paragraph, we evaluate the effects of DMAc from the comparison of T_{1C}s of the cellulose samples shown in Table 2.

In the DMAc-treated samples (samples A, C, D, and F), the signals at 106 ppm have the longer T_{1C}s than those in the other samples. On the other hand, T_{1C} of the signal at 84 ppm in the DMAc-treated cellulose is a little shorter than the other samples. Aside from these results, no significant difference was observed in the T_{1C}s of the signals at 90 (crystalline C-4), 66 (crystalline C-6), and 63 ppm (noncrystalline C-6). These results show that the DMAc treatment exerts the different effects on the magnetic relaxation phenomena of the respective carbons in an anhydroglucose unit. As it is supposed that the carbons in an anhydroglucose unit are in a different state due to the complex supramolecular structure of cellulose itself, the effects of the DMAc treatment on each carbon may be exerted in the different ways. Therefore, before we discuss the effect of the DMAc treatment on the mobility of cellulose molecule, we must consider the structural aspects that affect the T_{1C} of each carbon.

First, we consider the T_1 of the C-6 carbons. The existence of the relaxation component with the T_{1C} on the order of 100 s in the upfield C-6 signal shows that the molecular motion in some parts of the noncrystalline region is highly restricted. On the other hand, the downfield C-6 resonance, as well as the upfield one, contains the relaxation components with the T_{1C} of less than 1 s. This shows that the molecular motion in some of the crystalline region is considerably activated. Therefore, it can hardly be said that these relaxation components are simply assigned to the crystalline or the amorphous components. That is, the components have various degrees of molecular packing order: one possible explanation is that the differences in T_{1C} come from an inter- and/or intramolecular interaction, such as a hydrogen bond. It is supposed from this context that the relaxation component with the T_{1C} of 100 s of the C-6 resonance line is assigned to the carbons having a hydrogen-bonded hydroxyl group. Similarly, the relaxation components with the shorter T_{1C} are assigned to the C-6 carbons having a partially or nonhydrogen-bonded hydroxyl group. This seems inconsistent with the results obtained by Maréshal and Chanzy[21] from the FTIR measurements that the hydroxymethyl groups in native cellulose have three conformations corresponding to the hydrogen-bonding state. In the cellulose samples A to D, the relaxation component with the T_{1C} of less than 1 s had the major contribution to the overall relaxation of C-6 resonance line at 63 ppm. This suggests that most of the hydroxyl groups adjacent to the C-6 carbon in these cellulose samples are not hydrogen bonded. On the other hand, in the samples E and F, the relaxation component with the T_{1C} of several seconds mainly comprised the relaxation profile at 63 ppm. This implies that most of the hydroxyl groups adjacent to the C-6 carbon in these cellulose samples are partially hydrogen bonded. The above explanation on the relaxation behavior observed at the C-6 resonance lines can also be applied for the multiplicity in the chemical shift and the relaxation behavior of the C-4 resonances at 90 and 84 ppm. In the previous studies, these signals were assigned to the structural components with a different conformational regularity[14] or with a different hydrogen-bonding state.[30] However, the dynamic aspects of these structural components have not been clarified yet. In our experiments, both the C-4 signals have multiple relaxation components. This suggests that the carbons adjacent to the hydroxyl groups with the different hydrogen-bonding states are contained both in the structural components with the ordered and the disordered conformation.

The above discussion on the hydrogen-bonding state in cellulose samples derived from T_{1C} relaxometry data in solid-state NMR spectroscopy is supported by the results obtained from FTIR spectroscopy. Among the cellulose samples compared, the DMAc-treated cellulose showed the lowest absorption intensities at 3458 and 3267 cm^{-1}. Both these absorptions are assigned to the stretching of the hydrogen-bonded OH group adjacent to the C-2 carbon. On the other hand, the absorption at 3336 cm^{-1}, assigned to the stretching of the OH-3 forming a hydrogen bond with the O-5 oxygen atom, was the strongest in the DMAc-treated cellulose. These results suggest that, contrary to the previous suggestion made by Kamide et al., the so-called 'intramolecular hydrogen bond'[30] between the OH-3 group and the O-5 oxygen atom is not related to the solubility of cellulose in LiCl/DMAc. It is rather likely that more hydrogen bonds are formed between OH-3 and O-5 in the DMAc-treated cellulose than in other cellulose samples. Instead, the breakage of the intermolecular hydrogen bond between OH-2 and O-6 seems more significant for the dissolution of cellulose in LiCl/DMAc.

In addition to the changes in the hydrogen-bonding state, the solvation of cellulose by DMAc even in the dried state seems to facilitate the dissolution of cellulose. It is readily supposed that DMAc molecules solvating

the cellulose molecular chain at the surface of solid cellulose facilitates the penetration of the LiCl/DMAc complex into the cellulose solid. A detailed investigation on the effects of remaining amides in the solvent-exchanged cellulose on the dissolution behavior in LiCl/amide systems will be reported in another paper.[31]

Acknowledgments

The authors thank Professor Dr. T. Yoshizaki at the Graduate School of Engineering, Kyoto University, for his kind support in the SAXS measurements. This work was supported by a Grant-in-Aid for Scientific Research (No.12460076) from the Ministry of Education, Science, Sports, and Culture of Japan.

References

1. Turbak, A. F. *Tappi J.* **1984**, *67*, 94–96.
2. McCormick, C. L.; Callais, P. A.; Hutchinson, B. H., Jr. *Macromolecules* **1985**, *18*, 2394–2401.
3. Matsumoto, T.; Tatsumi, D.; Tamai, N.; Takaki, T. *Cellulose* **2002**, *8*, 275–282.
4. Aono, H.; Tatsumi, D.; Matsumoto, T. *Biomacromolecules* **2006**, *7*, 1311–1317.
5. Aono, H.; Tatsumi, D.; Matsumoto, T. *J. Polym. Sci. Part B: Polym. Phys.* **2006**, *44*, 2155–2160.
6. Yanagisawa, M.; Isogai, A. *Biomacromolecules* **2005**, *6*, 1258–1265.
7. Heinze, T.; Leibert, T. *Prog. Polym. Sci.* **2001**, *26*, 1689–1762.
8. Pionteck, H.; Berger, W.; Morgenstern, B.; Fengel, D. *Cellulose* **1996**, *3*, 127–139.
9. Ishii, D.; Tatsumi, D.; Matsumoto, T. *Biomacromolecules* **2003**, *4*, 1238–1243.
10. Ishii, D.; Kanazawa, Y.; Tatsumi, D.; Matsumoto, T. *J. Appl. Polym. Sci.* **2007**, *103*, 3976–3984.
11. Philipp, H. J.; Nelson, M. L.; Ziifle, H. M. *Textile Res. J.* **1947**, *17*, 585.
12. Teeäär, R.; Lippmaa, E. *Polym. Bull.* **1984**, *12*, 315–318.
13. Horii, F.; Hirai, A.; Kitamaru, R. *J. Carbohydr. Chem.* **1984**, *3*, 641–662.
14. Horii, F.; Hirai, A.; Kitamaru, R. *ACS Symp. Ser.* **1987**, *340*, 119–134.
15. Hirai, A.; Horii, F.; Kitamaru, R. *Cellulose Chem. Technol.* **1990**, *24*, 703–711.
16. Tsuboi, M. *J. Polym. Sci.* **1957**, *25*, 159–171.
17. Nelson, M. L.; O'Conner, R. T. *J. Appl. Polym. Sci.* **1964**, *8*, 1311–1324.
18. Nelson, M. L.; O'Conner, R. T. *J. Appl. Polym. Sci.* **1964**, *8*, 1325–1341.
19. Fengel, D. *Horzforschung* **1992**, *46*, 283–288.
20. Kondo, T.; Sawatari, C. *Polymer* **1996**, *37*, 393–399.
21. Maréshal, Y.; Chanzy, H. *J. Mol. Struct.* **2000**, *523*, 183–196.
22. Hayashi, H.; Hamada, F.; Suehiro, S.; Masaki, N.; Ogawa, T.; Miyaji, H. *J. Appl. Crystallogr.* **1988**, *21*, 330.
23. Torchia, D. A. *J. Magn. Reson.* **1978**, *30*, 613–616.
24. Schmidt, P. W. In *The Fractal Approach in Heterogeneous Chemistry*; Avnir, D., Ed.; John Wiley & Sons: Chichester, 1989; pp 67–79.
25. Axelson, D. E.; Russell, K. E. *Prog. Polym. Sci.* **1985**, *11*, 221–282.
26. Cheung, T. T. P.; Gerstein, B. C.; Ryan, L. M.; Taylor, R. E.; Dybowski, D. R. *J. Chem. Phys.* **1980**, *73*, 6059–6067.
27. Tanaka, H.; Nishi, T. *Phys. Rev.* **1986**, *B33*, 32–42.
28. http://www.molda.org/.
29. Durgaprasad, G.; Sathyanarayana, D. N.; Patel, C. C.; Randhawa, H. S.; Goel, A.; Rao, N. R. *Spectrochim. Acta, Part A* **1972**, *28*, 2311–2318.
30. Kamide, K.; Okajima, K.; Kowsaka, K. *Polym. J.* **1992**, *24*, 71–86.
31. Ishii, D.; Isogai, A. *Cellulose*, submitted for publication.